Relativistic Green's Function Model and Optical Potential*

Carlotta Giusti†

Dipartimento di Fisica, Università degli Studi di Pavia and INFN, Sezione di Pavia, via Bassi 6 I-27100 Pavia, Italy

Andrea Meucci

Dipartimento di Fisica Nucleare e Teorica, Università degli Studi di Pavia and INFN, Sezione di Pavia, via Bassi 6 I-27100 Pavia, Italy

Martin V. Ivanov

Institute for Nuclear Research and Nuclear Energy, Bulgarian Academy of Sciences, Sofia 1784, Bulgaria

José Manuel Udías

Grupo de Física Nuclear, Departamento de Física Atómica, Molecular y Nuclear, Universidad Complutense de Madrid, CEI Moncloa, 28040 Madrid, Spain

(Dated: March 21, 2016)

Abstract

The relativistic Green's function model describes final-state interactions in the inclusive quasi-elastic lepton-nucleus scattering by means of a complex optical potential. The model has been quite successfull in the description of data of electron and neutrino-nucleus scattering, but there are some caveats due to the use of phenomenological optical potentials. We discuss the theoretical uncertainties of the model and present results obtained with a new global relativistic folding optical potential.

INTRODUCTION

Accurate predictions of neutrino-nucleus cross sections are needed for use in experimental studies of neutrino oscillations, where nuclei are used as neutrino detectors. A proper analysis of data requires that uncertainties on nuclear effects in the response to neutrino interactions are reduced as much as possible. Several decades of experimental and theoretical work on electron scattering have provided a lot of detailed information on nuclear structure and dynamics [1, 2]. Models developed and successfully tested in comparison with electron-scattering data for electron scattering have been extended to neutrino-nucleus scattering. Although different, the two situations present many similar aspects and the comparison with electron-scattering data represents the first necessary test of a nuclear model. Recently, the MiniBooNE collaboration has produced high-quality data, mostly on a carbon target, for a number of selected channels, in particular, for the Quasi-Elastic (QE) one [3, 4], that is, where no pions are detected in the final state. Within the QE kinematic domain, the nuclear response to the electroweak probe is dominated by the process where, in the Impulse Approximation (IA), the probe directly interacts through a one-body current on a quasi-free nucleon which is then knocked out of the nucleus. A proper description of the Final-State Interactions (FSI) between the emitted nucleon and the residual nucleus is very important for a correct interpretation of the experimental data.

In electron-scattering experiments the emitted nucleon can be detected in coincidence with the scattered electron. Kinematic situations can be envisaged where the residual nucleus is left in a discrete eigenstate and the final state is completely determined. This is the exclusive one-nucleon knockout, that is usually described in the Distorted-Wave IA (DWIA), where FSI are accounted for by a complex Optical Potential (OP) whose absorptive imaginary part gives a reduction that is essential to reproduce $(e, e'p)$ data [1, 2, 5–8]. In the inclusive scattering, where only the scattered electron is detected, all the available final

nuclear states are included in the measured cross section. In this case, a model based on the DWIA, where the cross section is given by the sum, over all the nucleons, of integrated one-nucleon knockout processes and FSI are described by a complex OP with an imaginary absorptive part, is conceptually wrong. The OP describes elastic nucleon-nucleus and its imaginary part accounts for the fact that, if other channels are open besides the elastic one, part of the incident flux is lost in the elastically scattered beam and appears in the inelastic channels which are open. This flux may not contribute to the experimental cross section of the exclusive reaction, where only one channel is considered, and the experimental signal receives contributions mainly from the process where the knocked-out nucleon scatters elastically with the residual nucleus in the considered final state. In contrast, in the inclusive scattering the flux lost in a channel must be recovered in the other channels and in the sum over all the channels the flux can be redistributed but must be conserved. The DWIA does not conserve the flux.

In the Relativistic Green's Function (RGF) model FSI are described in the inclusive QE scattering consistently with the exclusive scattering by the same complex OP, but in the inclusive scattering the imaginary part redistributes and conserves the flux in the sum over all the final-state channels. The model was developed within a nonrelativistic [9, 10] and a relativistic framework [11–14] for the inclusive (e, e') scattering. The relativistic model (RGF) was extended to neutrino-nucleus scattering [15–23]. The formalism can translate the flux lost toward inelastic channels, represented by the imaginary part of the OP, into the strength observed in inclusive reactions. Therefore, the OP becomes a powerful tool to include important contributions not included in other descriptions of FSI based in the IA. The model has been quite successful in the comparison with data: it provides a good description of QE (e, e') data and of the Charged-Current QE (CCQE) MiniBooNE and MINERνA data, both for ν and $\bar{\nu}$ scattering [3, 4, 17, 19, 23–25], and of Neutral-Current Elastic (NCE) MiniBooNE data [18, 22, 26, 27].

The model is successfull but there are some caveats. Available phenomenological OPs make RGF calculations feasible, but do not allow us to disentangle and evaluate the role of a specific contribution: all inelastic contributions are included in the imaginary part of the OP. Phenomenological OPs are obtained through a fit to elastic proton-nucleus scattering data. Available data, however, do not completely constrain the shape and the size of the OP. Different OPs, able to give equivalent descriptions of elastic proton-scattering data, differ, in particular, in their imaginary parts, and therefore their inelastic contributions, and may produce theoretical uncertainties on the numerical predictions of the RGF model.

In this contribution we discuss the uncertainties due to the use of the OP in RGF calculations. In particular, we present results obtained with a new microscopic Global Relativistic Folding OP (GRFOP) [28, 29] generated within the Relativistic IA (RIA) by folding the Horowitz-Love-Franey (HLF) [30, 31] t-matrix with the relevant relativistic mean-field Lorentz densities via the so-called $t\rho$-approximation. The new results are compared with previous results obtained with phenomenological OPs [32].

RELATIVISTIC GREEN'S FUNCTION MODEL

Lepton-nucleus scattering is usually described in the one-boson exchange approximation, where the cross section is obtained from the contraction between the lepton tensor, which essentially depends on the lepton kinematics, and the hadron tensor $W^{\mu\nu}$, whose components are given by products of the matrix elements of the nuclear current between the initial and final nuclear states.

In the RGF model, with suitable approximations, mainly related to the IA, the components of the hadron tensor are written in terms of the s.p. optical model Green's function and then, exploiting the spectral representation of the s.p. Green's function, in a form containing matrix elements of the same type as the DWIA ones of the exclusive scattering, but where there are eigenfunctions of OP and of its Hermitian conjugate, where the imaginary part has an opposite sign and gives in one case an absorption and in other case a gain of strength. Therefore, in the model the imaginary part of the OP redistributes the flux lost in a channel in the other channels, and in the sum over all the channels the total flux is conserved. In the inclusive scattering, where all elastic and inelastic channels are included, the RGF formalism makes it possible to reconstruct the flux lost into nonelastic channels starting from the complex OP that describes elastic nucleon-nucleus scattering data. The model gives a good description of the experimental (e, e') cross sections in the QE region [11, 13, 14] and is able to describe CCQE and NCE MiniBooNE data and CCQE MINERνA data [17–19, 22, 23]. In comparison with the MiniBooNE cross sections, the RGF results are usually larger than the results of other models based on the IA, which, in general, underpredict data. The enhancement can be ascribed to the contribution of inelastic channels, which are recovered by the imaginary part of the OP and that are not included in other IA-based models.

The OP can recover contributions beyond direct one-nucleon emission, such as, for instance, rescattering of the outgoing nucleon and some multinucleon processes, which can be included in CCQE measurements. The model, being based on the use of a one-body nu-

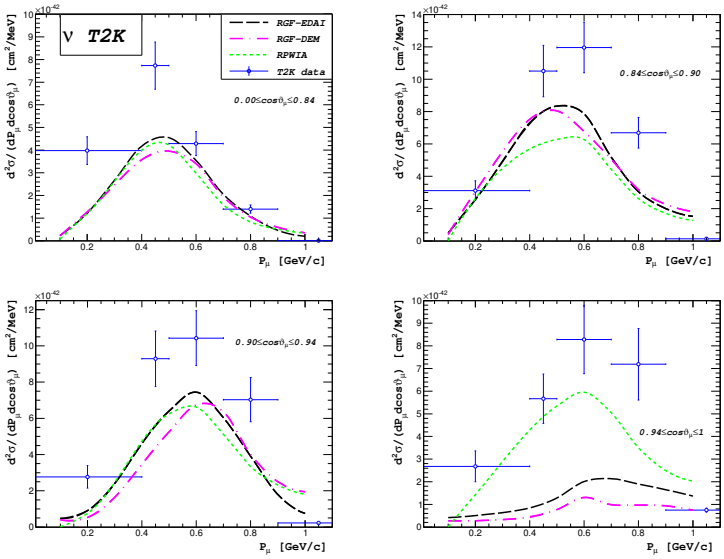

Figure 1: Flux-averaged CC-inclusive double differential ν_μ-^{12}C cross sections per target nucleon as a function of the muon momentum. The data are from T2K [34].

clear current, does not contain meson-exchange-currents mechanisms, that can be included in CCQE data, On the other hand, the OP can include pion-absorption and pion-emission processes, that should have already been subtracted in CCQE data. With a phenomenological OP we cannot disentangle the role of a specific reaction process. It has been written in [33] that the good agreement of the RGF results with the MiniBooNE data "should be interpreted with care" and that "it would be very interesting to confront the RGF results with the fully CC-inclusive data", where pion production is included.

The comparison with the fully CC-inclusive cross sections on ^{12}C measured by the T2K collaboration [34] is shown in Fig. 1. For the RGF calculations, two different parametrizations for the OP of ^{12}C have been adopted: the Energy-Dependent and A-Independent EDAI OP of [32] and the Democratic (DEM) OP of [35]. EDAI is a single-nucleus parametrization, which is constructed to better reproduce the elastic proton-^{12}C phenomenology, whereas DEM is obtained through a fit to elastic proton scattering data on a wide range of nuclei. The results of the Relativistic Plane-Wave IA (RPWIA), where FSI are neglected, also shown in the figure, are approximately 50% lower than the data. Both RGF results are also generally lower than the data, although within the error bars for low values of the muon momentum and large angular bins. In the RGF the imaginary part of the OP can include the excitation of multinucleon channels, it may contain some contribution due to pion emission, but the results in Fig. 1 clearly show that this is not enough to reproduce

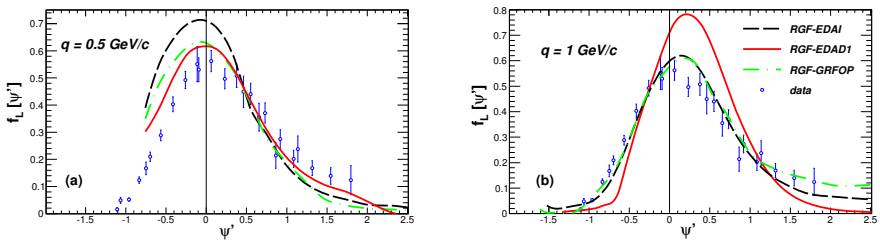

Figure 2: Longitudinal contributions to the scaling function for $q = 500$ and 1000 MeV/c compared with the averaged experimental scaling function.

CC-inclusive data. [36].

GLOBAL RELATIVISTIC FOLDING OPTICAL POTENTIAL

To reduce the uncertainties on the RGF results due to the use of phenomenological OPs, the need arises to build microscopic OPs. A new relativistic OP has been built for ^{12}C, a nucleus that is often used in neutrino-scattering experiments. The new OP is global, i.e., spanning a large range of kinetic energies of the nucleon, and it has been built within the RIA, by folding [28, 29] the HLF t-matrix [30, 31] with the relativistic mean-field Lorentz densities via the so-called $t\rho$-approximation. In this way the shape of the OP is severely constrained by the assumed shape of the nuclear density and the strength of the different contributions is essentially dictated by their respective contents in the effective parametrization of the NN scattering amplitudes. The new GRFOP: 1) is derived from all available data of elastic proton scattering on ^{12}C we are aware of; 2) stems from a folding approach, with neutron density fitted to data and proton density taken from electron-scattering experiments; 3) the same nuclear densities are used at all the energies in the range between 20 and 1040 MeV; 4) the imaginary term is built from the effective NN interaction.

The GRFOP reproduces quite well the experimental cross sections and analyzing powers for the elastic proton scattering on ^{12}C in the energy range between 20 and 1040 MeV [29], with an agreement comparable to the one obtained with the EDAI and EDAD1 OPs [32].

The GRFOP has been tested within the RGF for QE electron scattering and $\nu(\bar{\nu})$-nucleus scattering at MiniBooNE kinematics [29]. In the case of electron scattering, the results are in generally good agreement with the experimental (e, e') cross sections and close to the results obtained with EDAI and EDAD1 [29]. Of particular interest is the comparison with the experimental longitudinal scaling function. The analysis of QE (e, e') world data has

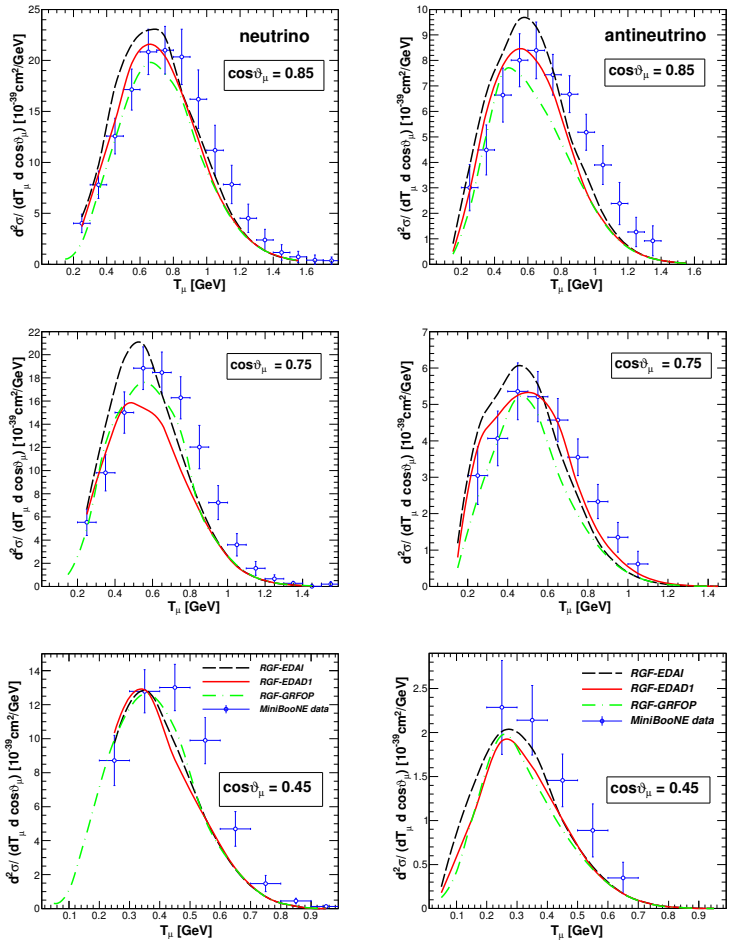

Figure 3: Flux-averaged double-differential cross section per target nucleon for the CCQE $^{12}\mathrm{C}(\nu_\mu, \mu^-)$ (left panels) and $^{12}\mathrm{C}(\bar{\nu}_\mu, \mu^-)$ (right panels) reactions as a function of the muon kinetic energy T_μ for three bins of the muon scattering angle $\cos\vartheta_\mu$ calculated with RGF-GRFOP (dot-dashed lines), RGF-EDAD1 (solid lines) and RGF-EDAI (dashed lines). Experimental data from MiniBooNE [3, 4].

shown that these data, when plotted against a properly chosen scaling variable Ψ', show a mild dependence on the momentum transfer (scaling of first kind) and almost no dependence on the nuclear target (scaling of second kind). These properties are well satisfied in the longitudinal channel, while violations associated to effects beyond the IA occur mainly in the transverse channel [37, 38]. The scaling function is obtained dividing the longitudinal contribution to the (e, e') cross sections by an appropriate single-nucleon cross section [37, 39]. In Fig. 2 the scaling functions obtained in the RGF with the RGFOP, EDAI, and EDAD1 OPs for two values of the momentum transfer q are compared with the experimental function.

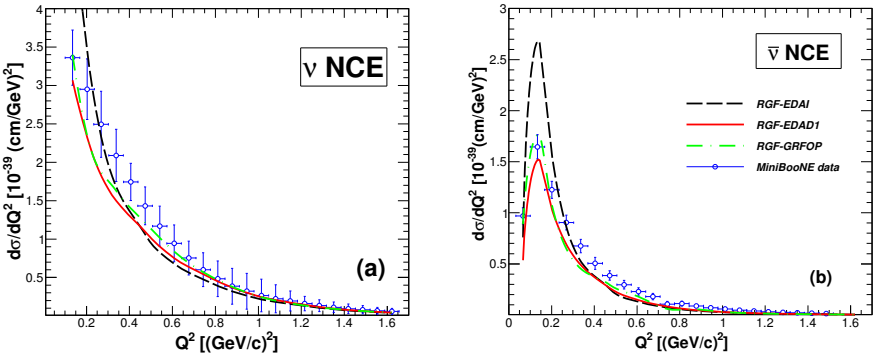

Figure 4: (Neutrino and antineutrino NCE flux-averaged cross section per target nucleon as a functions of Q^2 calculated with RGF-GRFOP (dot-dashed lines), RGF-EDAD1 (solid lines), and RGF-EDAI (dashed lines). Experimental data from MiniBooNE [26, 27].

The asymmetric shape of the experimental function is reproduced by the RGF model. The different dependence on q of the results with the three OPs makes the RGF scaling-function tail less pronounced as the value of q goes up. It is interesting to notice the different behavior as a function of q of the results with EDAI and EDAD1 in comparison with the experimental function: EDAD1 reproduces the experimental function at $q = 0.5$ GeV/c and overestimates it at $q = 1$ GeV/c, while with EDAI the experimental function is overestimated at $q = 0.5$ GeV/c and reproduced at $q = 0.5$ MeV/c. The RGF results with these two OPs do no scale enough. In contrast, the results with RGFOP scale better, they give a milder dependence on q and a better agreement with the experimental scaling function.

The comparison with the CCQE MiniBooNE data is presented in Fig. 3 for three bins of the muon scattering angle. A good agreement with the shape of the experimental cross sections is generally obtained with all the three OPs. The RGF-EDAD1 and RGF-EDAI results are similar in the bin $0.4 \leq \cos\vartheta_\mu \leq 0.5$. Larger differences, around 20%, are obtained in the peak region for the forward-angle scattering bins, the RGF-EDAI results being larger than the RGF-EDAD1 ones and in somewhat better agreement with the ν-scattering data. In the case of $\bar{\nu}$ scattering, data are sligthly overestimated by RGF-EDAI and satisfactorily described by RGF-EDAD1. The RGF-GRFOP results are always smaller that the RGF-EDAI and the RGF-EDAD1 ones for the bin $0.8 \leq \cos\vartheta_\mu \leq 0.9$, while for the bin $0.7 \leq \cos\vartheta_\mu \leq 0.8$ they are larger than the RGF-EDAD1 results and in better agreement with the data. Similar results in comparison with data are produced by the three RGF calculations for the bin $0.4 \leq \cos\vartheta_\mu \leq 0.5$.

The MiniBooNE collaboration has also measured the NCE flux-averaged differential ν and

$\bar{\nu}$ cross section on CH_2 as a function of the four-momentum transferred squared Q^2 [26, 27]. The comparison with the RGF results is shown in Fig. 4. For ν scattering the RGF-EDAI results reproduce the shape and the magnitude of the experimental cross section, but overestimate the first datum at the smallest value of Q^2; the RGF-EDAD1 results understimate the data only at the smallest values of Q^2; the RGF-GRFOP calculations generally provide a satisfactory agreement with the data. Also for $\bar{\nu}$ scattering the RGF results are in satisfactory agreement with the data. Close results are obtained with RGF-EDAD1 and RGF-GRFOP, while the RGF-EDAI cross section is enhanced at $Q^2 \approx 0.1$ (GeV/c)^2. All the RGF results reproduce the first datum at $Q^2 \approx 0.06$ (GeV/c)^2.

The RGF-GRFOP results lie, in general, between the RGF-EDAI and RGF-EDA1 ones and are in many cases in better agreement with the data. The new GRFOP results reduce the uncertainties in the numerical predictions of the RGF model and confirm our previous findings in comparison with data. The RIA can provide successful relativistic OPs with similar fits to elastic nucleon-nucleus scattering data. The GRFOP can be employed as a useful alternative to phenomenological optical potentials.

---

* *Presented at NuFact15, 10-15 Aug 2015, Rio de Janeiro, Brazil [C15-08-10.2]*

† carlotta.giusti@pv.infn.it; Speaker

[1] S. Boffi, C. Giusti, and F.D. Pacati, *Phys. Rep.* **226** (1993) 1-101.

[2] S. Boffi, C. Giusti, F.D. Pacati, and M. Radici *Electromagnetic Response of Atomic Nuclei* Oxford Studies in Nuclear Physics, Vol. 20, Clarendon Press, Oxford (1996).

[3] A.A. Aguilar-Arevalo *et al.*, *Phys. Rev.D* **81** (2010) 092005-1-22.

[4] A.A. Aguilar-Arevalo *et al.*, *Phys. Rev.D* **88** (2013) 032001-1-22.

[5] J.M. Udías *et al.*, *Phys. Rev. C* **48** (1993) 2731-2739.

[6] A. Meucci, C. Giusti, and F.D. Pacati, *Phys. Rev.C* **64** (2001) 014604-1-10.

[7] A. Meucci, C. Giusti, and F.D. Pacati, *Phys. Rev.C* **64** (2001) 064615-1-8.

[8] C. Giusti *et al.*, *Phys. Rev.C* **84** (2011) 024615-1-12.

[9] F. Capuzzi, C. Giusti, and F.D. Pacati *Nucl. Phys.A* **524** (1991) 681-705.

[10] F. Capuzzi *et al.*, *Ann. Phys.* **317** (2005) 492-529.

[11] A. Meucci *et al.*, *Phys. Rev.C* **67** (2003) 054601-1-12.

[12] A. Meucci, C. Giusti, and F.D. Pacati *Nucl. Phys. A* **756** (2005) 359-381.

[13] A. Meucci *et al.*, *Phys. Rev. C* **80** (2009) 024605-1-12.

[14] A. Meucci *et al.*, *Phys. Rev. C* **87** (2013) 054620-1-14.

[15] A. Meucci, C. Giusti, and F.D. Pacati *Nucl. Phys. A* **739** (2004) 277-290.

[16] A. Meucci *et al.*, *Phys. Rev. C* **83** (2011) 064614-1-10.

[17] A. Meucci *et al.*, *Phys. Rev. Lett.* **107** (2011) 172501-1-5.

[18] A. Meucci, C. Giusti, and F.D. Pacati, *Phys. Rev. D* **84** (2011) 113003-1-8.

[19] A. Meucci, and C. Giusti, *Phys. Rev. D* **85** (2012) 093002-1-6.

[20] A. Meucci, C. Giusti, and M. Vorabbi, *Phys. Rev. D* **88** (2013) 013006-1-7.

[21] R. González-Jiménez *et al.*, *Phys. Rev. C* **88** (2013) 025502-1-10.

[22] A. Meucci, and C. Giusti, *Phys. Rev. D* **89** (2014) 057302-1-4.

[23] A. Meucci, and C. Giusti, *Phys. Rev. D* **88** (2014) 117301-1-5.

[24] G.A. Fiorentini *et al.*, *Phys. Rev. Lett.* **111** (2013) 022502-1-6.

[25] L. Fields *et al.*, *Phys. Rev. Lett.* **111** (2013) 022501-1-7.

[26] A.A. Aguilar-Arevalo *et al.*, *Phys. Rev.D* **82** (2010) 092005-1-16.

[27] A.A. Aguilar-Arevalo *et al.*, *Phys. Rev.D* **91** (2015) 092005-1-12.

[28] M.V. Ivanov *et al.*, *Nuclear Theory* **30** (2011) 116-125, eds. A.I. Georgieva and N. Minkov, Heron Press, Sofia.

[29] M.V. Ivanov *et al.*, *Phys.Rev. C* to be published.

[30] C.J Horowitz, *Phys. Rev. C* **31** (1985) 1340-1348.

[31] D.P. Murdock and C.J Horowitz, *Phys. Rev. C* **35** (1987) 1442-1462.

[32] E.D. Cooper *et al.*, *Phys. Rev.C* **47** (1993) 297-311.

[33] L. Alvarez-Ruso, Y. Hayato, and J. Nieves, *New. J. Phys* **16** (2014) 075015-1-63.

[34] K. Abe *et al.*, *Phys. Rev. D* **87** (2013) 092003-1-20.

[35] E.D. Cooper, S. Hama, and B.C. Clark, *Phys. Rev.C* **80** (2009) 034605-1-5.

[36] A. Meucci and C. Giusti, *Phys. Rev.D* **91** (2015) 093004-1-6.

[37] C. Maieron, T.W. Donnelly, and I. Sick, *Phys. Rev. C* **65** (2002) 025502-1-15.

[38] T.W. Donnelly and I. Sick, *Phys. Rev. Lett.* **82** (1999) 3212-3215.

[39] J.A. Caballero, *Phys. Rev. C* **74** (2006) 015502-1-12.